Text S1: PROFILE calculations

The computed diffusive flux (flux PS, Eq. 1) across the sediment water interface (SWI) and depth resolved volumetric consumption rate (R_V, Eq. 2) were computed for each oxygen microprofile using the model PROFILE as described in Berg et al., (1998). PROFILE requires inputs for porosity (ϕ), free solute and sediment diffusivity (D_0 and D_S, respectively), and relevant boundary conditions for solute concentrations and/or fluxes. Due to macrofauna being removed from the cores, sediment bioturbation and irrigation were of negligible importance, and were therefore excluded from model calculations. All PROFILE inputs and computation notes are detailed in Table S1.

$$flux\ PS = \phi_0 D_{S,0} \left.\frac{\partial C}{\partial \mathrm{x}}\right|_{x=0^+} \qquad Eq.1$$

where C is the concentration, x is sediment depth, and $x = 0^+$ denotes the position just below the SWI (Glud, 2008; Rasmussen and Jorgensen, 1992). PROFILE fits constant R_V zones that best characterise the measured microprofiles numerically by reducing the number of R_V zones to achieve the simplest fit in line with the prescribed F-statistics (see Berg et al., 1998). In steady state, and under the assumption that sediment bioturbation and irrigation are of negligible importance, R_V can be defined as:

$$R_v = \frac{\partial}{\partial_{\mathrm{x}}} \left(\phi D_s \left(\frac{\partial C}{\partial \mathrm{x}} \right)_s \right) \qquad Eq.2$$

where S denotes the sediment domain. PROFILE requires the user to define a SWI and estimates of sediment porosity and diffusivity. Given the coarse resolution (200 μm) relative to the diffusive boundary layer (DBL) height, it difficult to precisely locate the SWI. Nevertheless, through a visual inspection of individual concentration microprofiles (Bryant et al., 2010), the SWI was identified as an inflection point in the upper region of the concentration gradient, where the diffusivity decreases due to tortuosity (Røy et al., 2004). In cases where inflection points were unclear, i.e., situations where sediment consumption was high or the turbulent mixing had not fully propagated above the diffusive boundary layer, the selection of the SWI was informed by the series of microprofiles (Bryant et al., 2010) that showed there were typically three intervals (600 µm) between the mixed layer and SWI. This adoption of the series approach was selected due to the controlled laboratory conditions likely resulting in a consistent DBL.

The sediment diffusivity in PROFILE was defined using Archie's Law (Eq. 3):

$$D_s = {\phi_0}^{m-1} D_0 \qquad Eq.3$$

where m is the sensitivity correction exponent selected based on sediment type (Ullman and Aller, 1982). For unlithified sediments, when $\phi \leq 0.7$, m = 2 is used versus in sediments where $\phi \geq 0.7$, then the sensitivity is greater and m = 2.5 to 3 is used (Ullman and Aller, 1982). A known bulk porosity (ϕ_d) of 0.71 was defined from cores using the wet (m_w) and dry (m_s) weight of homogenised surface sediments (upper 2 cm) (Eq. 4; Burdige, 2006),

$$\phi_d = \frac{m_w/\rho_w}{m_w/\rho_w + (m_s - S_{m_s})/\rho_s} \qquad Eq.4$$

where a water density (ρ_w) of 1.025 g cm^{-3}, sediment density (ρ_s) of 2.7 g cm^{-3}, and salinity (S) of 35.2 g kg^{-1} were used. As such, due to $\phi_0 > \phi_d = 0.71$, m = 3 was applied.

PROFILE computed fluxes (flux PS) were assessed next to free solution flux estimates given by $D_0 \frac{\partial C}{\partial \mathrm{x}}$ for three intervals nearest to the SWI (Figures S1 and S2): the first (purple) was above the SWI and assumed to only encompass the water column; the second (yellow) was assumed to be immediately above, if not encompass, the SWI; and the third (green), was assumed to encompass sediment only.

Flux PS consistently underestimated the diffusive uptake defined by the free solution flux estimates when a constant bulk porosity was applied. For example, Flux PS assuming a single porosity was 174 μmol m^{-2} h^{-1} was well below all the free solution flux estimates of 328 and 237μmol m^{-2} h^{-1} for yellow and purple intervals, respectively (Figure S1). This discrepancy of diffusive estimates was largely remedied after we applied a sediment porosity gradient to the upper sediment layer in PROFILE, similar to porosity decay profiles reported in Ternat et al., (2008) and Vopel et al., (2009). To do this, Athy's law (Eq. 5) was applied:

$$\phi_{sand}(x) = \phi_d + (\phi_0 - \phi_d)e^{-x/b_p} \qquad Eq.5$$

where x is profile depth, ϕ_0 and ϕ_d are the surface porosity and bulk porosity, respectively, and bp is the porosity depth decay scale (assumed to be 1 mm).

Athy's law assumes, $\phi_d < \phi_0$, as such, an unknown surface porosity had to be determined. By assuming the conservation of oxygen flux at the SWI (Eq. 6, Jørgensen et al., 2022).

$$D_0 \frac{\partial C}{\partial x}\Big|_{x=0^-} = \phi_0 D_S \frac{\partial C}{\partial x}\Big|_{x=0^+} \qquad Eq.6$$

where $x = 0^-$ denotes the interval just above the SWI. Surface porosity was calculated to be $\phi_0 = 0.9$, however, due to the uncertainty of the "large" intervals potentially encompassing boundaries (i.e., SWI, or mixed layer above the DBL), surface porosity values ± 10% were also considered. Frequent overestimation of the oxygen uptake by the PROFILE DOU using >0.85, led to a surface porosity of 0.85 to be used in PROFILE for all uncovered microprofiles (no bacterial mats visible), resulting in a typical model fit greater than $R^2 = 0.9998$ and Flux PS within the free solution flux estimates (Figure S2).

For microprofiles in bacterial biofilms (covered sediments), porosity was defined differently in PROFILE. Bacterial biofilms were assumed to be motile, positioning themselves at the interface of oxygen and reduced solutes (Bernard and Fenchel, 1995; Fenchel and Glud, 1998). This means that the inflection point identified in each microprofile, where the diffusivity decreases due to tortuosity (Røy et al., 2004), was likely identifying the surface of the biofilms instead of the surface of the sediments. Occasionally, due to the higher porosity and consumption rates, this first inflection point was difficult to distinguish, and in those cases, a DBL of 0.6 mm was assumed to be consistent with uncovered microprofiles. It was also assumed that oxygen would largely be depleted above the sediment surface where white biofilms were present (Schulz and Jørgensen, 2001). the sediment surface, or base of the biofilm, was not apparent in the microprofiles due to the 200 µm interval scale and low oxygen concentrations obscuring any second inflection. This inability to identify the base of biofilms is unlikely to affect DOU rates, as rates are unaffected by biofilm thickness >0.2 mm, and in previous studies, thinly veiled to fibrous biofilms ranged from 0.2 to 0.6 mm (Bernard and Fenchel, 1995; Fenchel and Bernard, 1996). A constant porosity of $\phi_G = 0.95$ and diffusivity for m = 3 (Bernard and Fenchel, 1995) were assumed for the fitted mat profile. We note that the relationship between porosity and diffusivity is not established for bacterial biomass, but that the formulation provides reasonable agreement between PROFILE calculations and the free solution flux estimates.

We acknowledge that the method we present here has limitations. However, the approach has reasonable foundation, and provides agreement among diffusive oxygen uptake estimates across the dataset of ~100 microprofiles.

Table S1. PROFILE model inputs

Input	Value	Notes	Source
Depth at top of calculation domain	0	DBL not included	
Depth at bottom of calculation domain	x_max	final measurement for replicate	measured
Max number of equally spaced zones	10		selected
Type of boundary conditions	4	concentration at SWI, zero flux at base	selected
First boundary condition	C_{SWI}	concentration at SWI	measured
Second boundary condition	0	zero flux at base	selected
Diffusivity in water (D) ($cm^2\ s^{-1}$)	1.957e-05	free solution at 20.2 °C, sal 35	1*
Expression for sediment diffusivity (D_S)	2	$D_S = \phi^2 D$	2*
Concentration in water column (C_0)	N/A	no irrigation	-
Minimum for production rate	-1e+20	nominal large negative	-
Maximum for production rate	0	insufficient light	selected
Maximum deviation for acceptance	0.001	default	3*
Level of significance in the F statistics	0.01	default	

1* Brecker & Peng (1974)

2* Ullman and Aller (1982)

3* Berg et al., (1998)

Additional computation notes:

Irrigation ($\alpha = 0$) and bioturbation ($D_B = 0$) due to removal of macrofauna

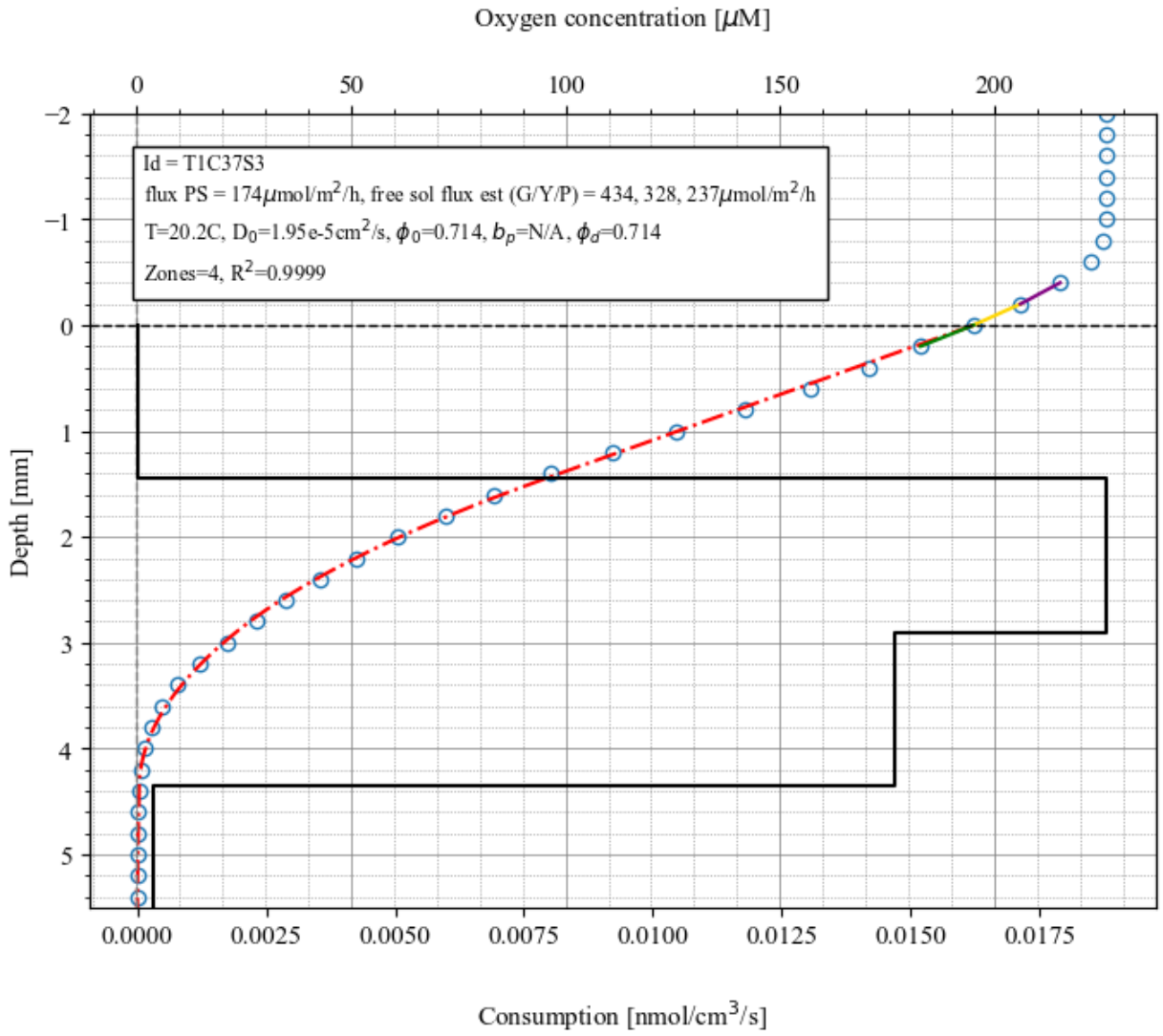

Figure S1. PROFILE model fit using constant porosity ϕ=0.714 (red dashed line). PROFILE computed flux (flux PS, 174 μmol m^{-2} h^{-1}) and free solution flux estimates given by $D_0\partial C/\partial x$ for intervals above the SWI (purple, 237 μmol m^{-2} h^{-1}), encompassing the SWI (yellow, 328 μmol m^{-2} h^{-1}), and below the SWI (green, 434 μmol m^{-2} h^{-1}). Depth resolved volumetric consumption rates are outline in black.

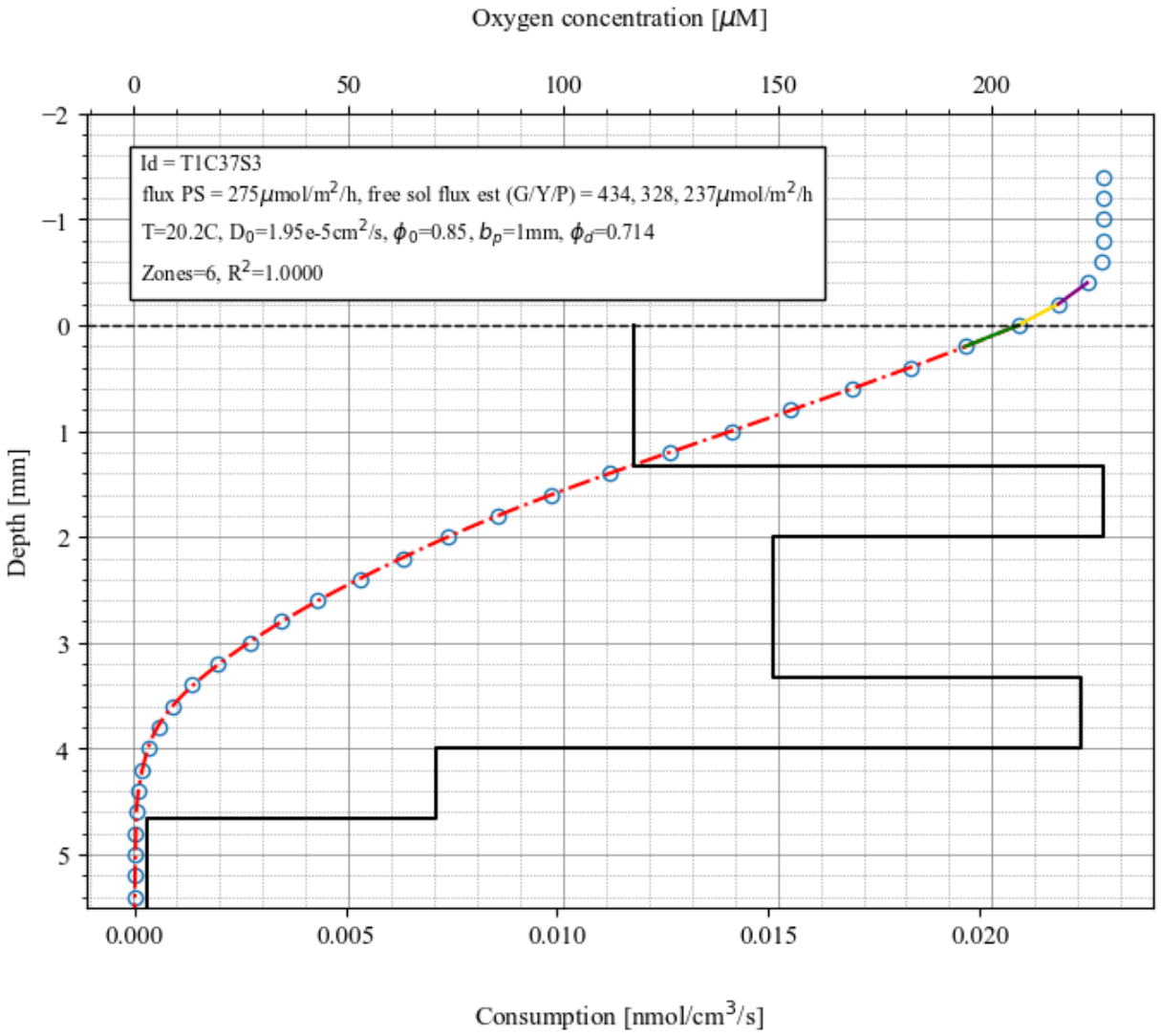

Figure S2. PROFILE model fit using porosity gradient for a microprofile in uncovered sediment (red dashed line). PROFILE computed flux (flux PS, 275 μmol m^{-2} h^{-1}) and free solution flux estimates given by $D_0 \partial C/\partial x$ for intervals above the SWI (purple, 237 μmol m^{-2} h^{-1}), encompassing the SWI (yellow, 328 μmol m^{-2} h^{-1}), and below the SWI (green, 434 μmol m^{-2} h^{-1}). Depth resolved volumetric consumption rates are outline in black.

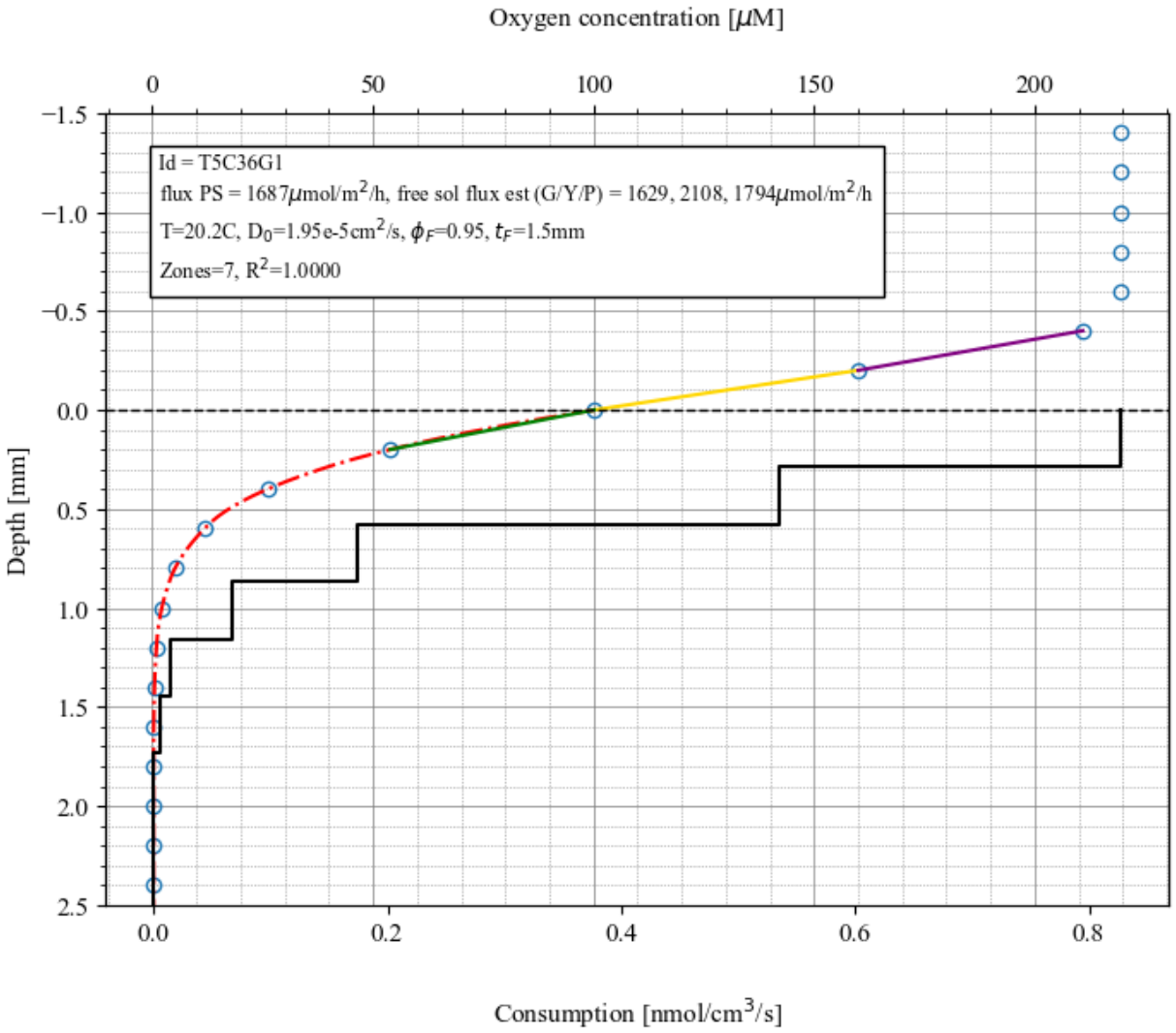

Figure S3. PROFILE model fit using constant porosity $\phi = 0.95$ for a microprofile in biofilm covered sediment (red dashed line). PROFILE computed flux (flux PS, 1687 μmol m^{-2} h^{-1}) and free solution flux estimates given by $D_0 \partial C/\partial x$ for intervals above the biofilm (purple, 1794 μmol m^{-2} h^{-1}), encompassing the biofilm (yellow, 2108 μmol m^{-2} h^{-1}), and below the biofilm (green, 1629 μmol m^{-2} h^{-1}). Depth resolved volumetric consumption rates are outline in black.

References

Berg, P., Risgaard-Petersen, N., Rysgaard, S., 1998. Interpretation of measured concentration profiles in sediment pore water. Limnol. Oceanogr. 43, 1500–1510. https://doi.org/10.4319/lo.1998.43.7.1500

Bernard, C., Fenchel, T., 1995. Mats of colourless sulphur bacteria. II. Structure, composition of biota and successional patterns. Mar. Ecol. Prog. Ser. 128, 171–179. https://doi.org/10.3354/meps128171

Bryant, L.D., Mcginnis, D.F., Lorrai, C., Brand, A., Little, J.C., Wüest, A., 2010. Evaluating oxygen fluxes using microprofiles from both sides of the sediment – water interface. Limnol. Oceanogr. Methods 8, 610–627. https://doi.org/10.4319/lom.2010.8.610

Fenchel, T., Glud, R.N., 1998. Veil architecture in a sulphide-oxidizing bacterium enhances countercurrent flux. Nature 394, 367–369. https://doi.org/10.1038/28609

Glud, R.N., 2008. Oxygen dynamics of marine sediments. Mar. Biol. Res. 4, 243–289. https://doi.org/10.1080/17451000801888726

Jørgensen, B.B., Wenzhöfer, F., Egger, M., Glud, R.N., 2022. Sediment oxygen consumption: Role in the global marine carbon cycle. Earth-Science Rev. 228. https://doi.org/10.1016/j.earscirev.2022.103987

Rasmussen, H., Jorgensen, B.B., 1992. Microelectrode studies of seasonal oxygen uptake in a coastal sediment: role of molecular diffusion. Mar. Ecol. Prog. Ser. 81, 289–303. https://doi.org/10.3354/meps081289

Røy, H., Huettel, M., Jørgensen, B.B., 2004. Transmission of oxygen concentration fluctuations through the diffusive boundary layer overlying aquatic sediments. Limnol. Oceanogr. 49, 686–692.

Schulz, H., Jørgensen, B.B., 2001. Big Bacteria. Molecules.

Ternat, F., Boyer, P., Anselmet, F., Amielh, M., 2008. Erosion threshold of saturated natural cohesive sediments: Modeling and experiments. Water Resour. Res. 44, 1–18. https://doi.org/10.1029/2007WR006537

Ullman, W.J., Aller, R.C., 1982. Diffusion coefficients in nearshore marine sediments. Limnol. Oceanogr. 27, 552–556. https://doi.org/10.4319/lo.1982.27.3.0552

Vopel, K., Pilditch, C.A., Wilson, P., Ellwood, M.J., 2009. Oxidation of surface sediment: Effects of disturbance depth and seawater flow speed. Mar. Ecol. Prog. Ser. 392, 43–55. https://doi.org/10.3354/meps08179